

# A METHOD FOR CARRIER FREQUENCY AND PHASE SYNCHRONIZATION OF TWO AUTONOMOUS COOPERATIVE TRANSMITTERS

*D. Richard Brown III, Gregory B. Prince, and John A. McNeill*

Department of Electrical and Computer Engineering  
Worcester Polytechnic Institute, Worcester, MA 01609

## ABSTRACT

Cooperative communication protocols in which two or more sources transmit simultaneously in a single subchannel offer the potential for increased power efficiency and achievable rate with respect to orthogonal transmit cooperation. These protocols are, however, complicated by the fact that they require strict transmitter synchronization in order for the carrier signals from each source to arrive in phase and constructively combine at the intended destination. This paper develops an explicit method for synchronizing the carriers of two sources in a cooperative communication system with one destination. Unlike the prior work in this area, the approach described in this paper allows for source and/or destination mobility. The performance of the proposed carrier synchronization system is investigated for several channel models and practical design considerations are also discussed.

## 1. INTRODUCTION

Of the various methods used to achieve reliable communications in wireless links, spatial diversity is particularly attractive in that it does not require any additional bandwidth or reduction in transmission rate. Spatial diversity does, however, require the use of multiple antennas which must be separated by at least a few wavelengths in order to be effective. This physical constraint precludes the use of spatial diversity in many scenarios such as cellular handsets.

Recently, researchers considered spatial diversity in the context of multiuser communication systems in which there may be multiple sources and/or destinations. Sendonaris, Erkip, and Aazhang were the first to suggest the concept of *user cooperation diversity* where nearby users in a cellular system form cooperative “partnerships” by sharing their antennas to achieve increased rate or decreased outage probability in the uplink [1]. User cooperation is motivated by the observation that the uplink signals in most communication systems are omnidirectional and that these signals could be received and acted upon by other users in the system.

Since the initial work in [1], much of the literature on user cooperation diversity has focused on the design of cooperative transmit protocols. All of the cooperative protocols operate in the general cooperative sense in that, once a source transmission has been received by a set of cooperating nodes, one or more of these nodes will transmit some amount of redundancy to the destination. The protocols specify how the cooperating sources convey this redundancy

to the destination. In almost all of the protocols, the redundancy either transmitted in an orthogonal subchannel, e.g. amplify-and-forward and decode-and-forward cooperation [2], or in a single subchannel, e.g. coherent cooperation [3, 4] and space-time coherent cooperation [5].

Single-subchannel coherent cooperative protocols offer the potential for increased power efficiency and achievable rate with respect to orthogonal subchannel cooperative protocols. These protocols are, however, complicated by the fact that they require strict transmitter synchronization in order for the carrier signals from each source to arrive in phase and constructively combine at the intended destination. This carrier synchronization problem was considered in the context of “distributed beamforming” in [6] where coherent combining is achieved through a master synchronization beacon and precise placement of both the source and destination nodes in order to equalize all round-trip propagation times. Mobility is not permitted in this system. A carrier synchronization scheme was also proposed in [7] where a beacon is used to measure round-trip phase delays between each transmitting node and the destination. The destination estimates and quantizes these phase delays and transmits them to the appropriate nodes for local phase pre-compensation. While this system does allow for some node mobility, the amount of mobility is restricted by the amount of time required to estimate, quantize, deliver, and implement the phase pre-compensation estimates.

This paper describes a new method for synchronizing the carriers of two sources in a cooperative communication system with one destination. Unlike [6, 7], the approach described in this paper allows for high rates of source and/or destination mobility. The performance of the proposed system is investigated for several channel models and practical design considerations are also discussed.

## 2. SYSTEM DESCRIPTION

The proposed two-source carrier synchronization scheme is shown in Figure 1. This system is similar to the prior work in [6, 7] in that a sinusoidal beacon at frequency  $\omega_0$  rad/s is transmitted by the destination node to the source nodes. Unlike the prior work, however, the source nodes in our proposed system do not use this beacon signal directly for carrier synchronization but, rather, each employ a primary frequency-synthesis PLL [8] tuned to the beacon frequency  $\omega_0$  to generate a low-power secondary sinusoidal beacon that is phase locked to the master beacon but at frequency  $\omega_1 = \frac{N_1}{M_1}\omega_0$  where  $N_1$  and  $M_1$  are integers. The

secondary beacons propagate between the sources to a secondary frequency synthesis PLL in each source tuned to  $\omega_1$ . The secondary frequency synthesis PLL in each source generates a carrier signal at frequency  $\omega_c = \frac{N_2}{M_2}\omega_1$  that is phase locked to the received secondary beacon signal. These carrier signals are then used to modulate the baseband signals for bandpass transmission of information to the destination.

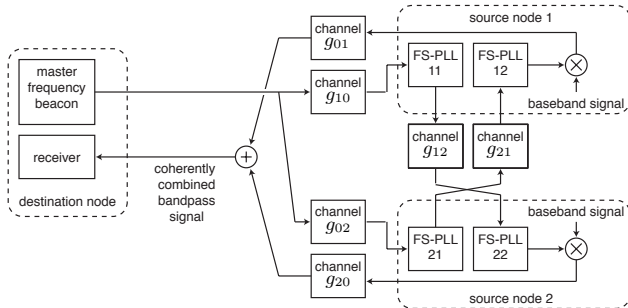


**Fig. 1.** Two-source carrier synchronization system model.

Assuming unmodulated carrier transmissions, the received signal at the destination can be written as

$$r(t) = a_1 \cos(\omega_c t + \phi_1) + a_2 \cos(\omega_c t + \phi_2)$$

where  $\phi_i$  and  $a_i$  are the received phase and amplitude, respectively, of the carrier signal from the  $i^{\text{th}}$  source. The power in the received signal is then

$$P_r = \frac{1}{2}(a_1^2 + 2a_1 a_2 \cos(\phi_\Delta) + a_2^2)$$

where  $\phi_\Delta := \phi_1 - \phi_2$  is the phase offset in the received carrier signals at the destination.

While we have placed no restrictions on the channels in Figure 1, the intuition behind the proposed carrier synchronization system is best exposed if we temporarily assume that all of the channels in the system are single-path and time-invariant. In this case, each channel is modeled as a propagation delay where the delay in the forward and reverse channel pair  $g_{ij}(t)$  and  $g_{ji}(t)$  is identical. Consequently, it can be shown that the total propagation time for the circuit  $D \rightarrow S_1 \rightarrow S_2 \rightarrow D$  is identical to the propagation time for the circuit  $D \rightarrow S_2 \rightarrow S_1 \rightarrow D$ . If the frequency synthesis PLLs in each source are designed to have identical phase shifts, the total phase shift through each circuit will be identical and  $\phi_\Delta$  will be equal to zero.

### 3. RESULTS

This section provides analysis and simulation examples of the proposed carrier synchronization system in three scenarios: time-invariant single-path channels, time-varying single-path channels, and time-varying multipath channels. The loop filter in each PLL is assumed to be of the form

$$F(s) = \frac{RC_2 s + 1}{RC_1 C_2 s^2 + C_2 s} \quad (1)$$

where  $R$ ,  $C_1$ , and  $C_2$  are chosen to achieve a specified loop bandwidth and phase margin. Denoting VCO sensitivity in rad/(s·V) as  $K_0$  and phase detector slope in V/rad as  $K_d$ ,

the closed loop phase transfer function of the PLL in the locked state is given as [8]

$$H(s) := \frac{\theta_{out}(s)}{\theta_{in}(s)} = \frac{K_0 K_d F(s) M^{-1}}{s + K_0 K_d F(s) N^{-1}}. \quad (2)$$

The results in this section assume that each PLL in the system employs an ideal VCO with sensitivity  $K_0 = 2\pi \cdot 10^5$  and a three-state phase-frequency detector [8] with slope  $K_d = 1$ . Unless otherwise specified, we also assume  $\omega_0 = 2\pi 800 \cdot 10^6$  rad/s,  $M_1 = M_2 = 1$ ,  $N_1 = N_2 = 2$ , and  $a_1 = a_2 = 1$ .

#### 3.1. Time-Invariant Single-Path Channels

We first consider the simplest scenario where all of the channels in the system are modeled as single-path channels with fixed delays and unity gain, i.e.,  $g_{ij} = g_{ji} = \delta(t - \tau_{ij})$ . Figure 2 shows a simulation of the carrier synchronization system in bandpass from an unlocked state to demonstrate convergence to the locked state in this scenario. In this example, all VCO center frequencies were set to ideal (Section 4.1.3 discusses the effect VCO center frequency inaccuracy), all initial VCO phases were randomly generated on  $[0, 2\pi)$ , and all channel delays  $\tau_{ij}$  were randomly generated. The loop filter bandwidths were set to 10 MHz in this example to facilitate rapid convergence to the locked state.

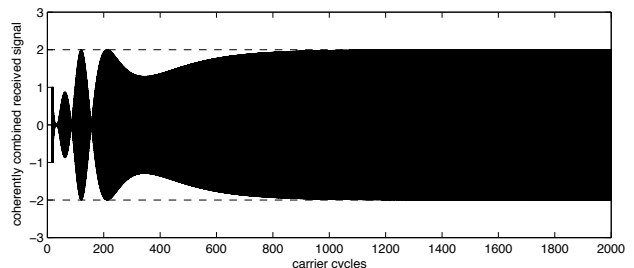


**Fig. 2.** Example of two-source carrier synchronization for time-invariant single-path channels.

This example demonstrates that the sources can achieve rapid carrier synchronization at the destination upon reception of the master beacon and is typical of the convergence behavior for different realizations of initial VCO phases and channel delays. The “lock-in time” is, roughly speaking, inversely proportional to the closed loop bandwidth of the PLLs [8]. A more modest closed loop bandwidth would increase the time required to achieve carrier synchronization but would also provide more robustness to noise.

#### 3.2. Time-Varying Single-Path Channels

In this section, we model all channels in the system as  $g_{ij} = g_{ji} = \delta(t - \tau_{ij}(t))$  where  $\tau_{ij}(t)$  varies due to movement of the sources and/or the destination. In this scenario, each PLL must track a time-varying input phase in order to generate a carrier that arrives with the desired phase at the destination.

To better understand the tracking capabilities of the system in this scenario, we consider a simple mobility model with piecewise-constant acceleration between  $D \leftrightarrow S_1$ ,  $D \leftrightarrow S_2$ , and  $S_1 \leftrightarrow S_2$ . The acceleration in each path is assumed

to be constant over an interval longer than several time constants of the PLLs' closed loop transfer functions. We use the convention that positive acceleration corresponds to attraction and negative acceleration corresponds to repulsion.

The piecewise-constant acceleration model implies linearly increasing/decreasing velocity which, in turn, implies that each PLL observes a frequency ramp at its input during an interval of constant acceleration. The slope of the frequency ramp at the input of the primary PLLs can be written as  $\Delta\dot{\omega}_{i1} = \alpha_{0i}\omega_0/c$  rad/s<sup>2</sup> where  $\alpha_{0i}$  is the acceleration in the path  $D \leftrightarrow S_i$  and  $c$  is the speed of light. The secondary PLLs must track the frequency ramp that results from acceleration the  $S_1 \leftrightarrow S_2$  path as well as the frequency ramp at the output of the primary PLL. Assuming that the primary PLLs are tracking, the slope of the frequency ramp at the input of the secondary PLLs can be written as  $\Delta\dot{\omega}_{j2} = \alpha_{12}\omega_1/c + \frac{N_1}{M_1}\Delta\dot{\omega}_{j1}$  rad/s<sup>2</sup> for  $j \neq i$ .

Using a linear model for the PLL, the steady-state phase error (at the PLL's internal frequency) of a PLL subjected to a frequency ramp input of slope  $\Delta\dot{\omega}$  is [8]

$$\theta_e(\infty) = \lim_{s \rightarrow 0} s \left[ 1 - \frac{M}{N} H(s) \right] \frac{\Delta\dot{\omega}}{Ms^3} = \kappa \Delta\dot{\omega} \frac{N}{M}$$

where  $\kappa = C_2(K_0K_d)^{-1}$  using the loop filter of (1). Mapping the internal phase errors of each PLL to the steady-state phase offset in the carriers arriving at the destination, it can be shown that

$$\phi_\Delta = (N_1\kappa_1 + N_2\kappa_2)(\alpha_{01} - \alpha_{02})\frac{\omega_c}{c} \quad (3)$$

for the piecewise-constant acceleration model where we have assumed that the primary and secondary PLLs have the same  $\kappa$  values ( $\kappa_1$  and  $\kappa_2$ , respectively). Note that (3) does not depend on mobility in the  $S_1 \leftrightarrow S_2$  path.

For a typical design of the loop filter (1), it can be shown that  $N_i\kappa_i$  is proportional to  $\omega_t^{-2}$  where  $\omega_t$  is the closed loop bandwidth of the PLL. Given a known carrier frequency  $\omega_c$ , a maximum acceleration specification, and a maximum tolerable phase offset in the received carriers, (3) implies a minimum closed loop bandwidth  $\omega_t$  for the PLLs to accurately track the phase dynamics that occur due to source and/or destination mobility. For typical values of maximum acceleration ( $\pm 9.8$  m/s<sup>2</sup>) and carrier frequency ( $< 10$  GHz), loop bandwidths on the order of 1 kHz lead to maximum received carrier phase offsets of less than one degree.

### 3.3. Time-Varying Multipath Channels

This section considers the performance of the proposed two-source carrier synchronization system in the case when the channels have multiple propagation paths. Time-invariant multipath channels simply introduce a fixed phase shift and gain to each sinusoidal signal in the system. Given a transmission frequency  $\omega$ , the channel phase shift  $\theta$  can be mapped to an "effective delay"  $\theta/\omega$ . For a general multipath channel, it is not reasonable to assume that the effective delay will be identical at two widely different frequencies, e.g.,  $\omega_0$  and  $\omega_c$ . Hence, it is not reasonable to assume that the overall round-trip delay through the proposed two-source carrier synchronization system will be identical in the

$D \rightarrow S_1 \rightarrow S_2 \rightarrow D$  and  $D \rightarrow S_2 \rightarrow S_1 \rightarrow D$  circuits for general multipath channels.

Nevertheless, to better understand how the performance of the system degrades from single-path to general multipath channels, we can consider the Ricean fading channel model where each channel in the system has one dominant specular or line-of-sight component and multiple scattered and reflected components. In the Ricean fading channel model, the specular component is modeled (in baseband) as a deterministic complex number and the sum effect of the scattered components is modeled as a zero-mean proper complex Gaussian random variable. The resulting phase shift of the Ricean channel can be written as

$$\theta = \theta_{LOS} + \Theta \quad (4)$$

where  $\theta_{LOS}$  is the deterministic phase of the dominant specular component and  $\Theta$  is the random phase perturbation caused by the scattered components of the channel. The distribution of  $\Theta$  can be shown to be [9]

$$f_\Theta(x) = \frac{e^{-K} \left\{ 1 + \sqrt{\pi K} e^{K \cos^2 x} \cos x \left[ 1 + \operatorname{erf}(\sqrt{K} \cos x) \right] \right\}}{2\pi}$$

where  $K$  is commonly called the Rice factor and represents the ratio of the power in the dominant specular component to the mean power in the scattered components.

Assuming that the time-variations of the channel are sufficiently slow such that any PLL phase tracking error is negligible, the resulting (random) carrier phase offset at the destination can be written as

$$\phi_\Delta = \frac{N_1 N_2}{M_1 M_2} \Theta_{01} - \Theta_{10} + \frac{N_1 N_2}{M_1 M_2} \Theta_{02} - \Theta_{20}$$

where  $\Theta_{0i}$  is the phase perturbation at  $\omega_0$  and  $\Theta_{i0}$  is the phase perturbation at  $\omega_c$ . We note that  $\Theta_{12}$  and  $\Theta_{21}$  do not contribute to the carrier phase offset since the  $S_1 \leftrightarrow S_2$  transmissions are at the same frequency and these channels can be assumed to be reciprocal. If we further assume that all of the  $\Theta_{ij}$  are i.i.d., the distribution of the carrier phase offset is only a function of the Rice factor  $K$ .

Figure 3 shows the effect of  $K$  on the statistics of the received power at the destination. To isolate the effect of the phase disturbances caused by the scattered components of the channels, the magnitude of each received carrier is normalized to unity, i.e.,  $a_1 = a_2 = 1$ . Figure 3 shows that, in cases when the power of the specular component is much greater than the scattered components ( $K \rightarrow \infty$ ), the channels are approximately single-path and the resulting received power is almost always very close to ideal. As  $K \rightarrow 1$ , the mean power in the scattered components approaches that of the specular component. In this regime, the scattered components of the multipath channels often cause large independent phase perturbations in the forward and reverse links. Figure 3 shows that these large phase perturbations cause the average received power at the destination to significantly diminish as  $K \rightarrow 1$ .

## 4. PRACTICAL CONSIDERATIONS

This section discusses practical considerations that may influence the realization of the proposed two-source carrier synchronization system shown in Figure 1.

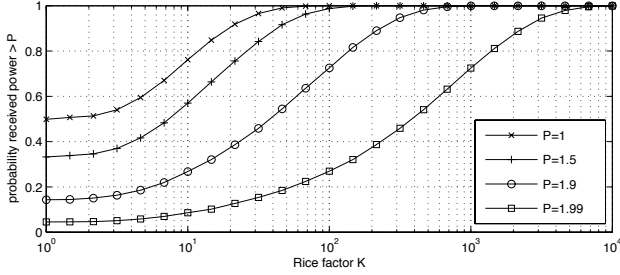


**Fig. 3.** Performance of the two-source carrier synchronization system for the baseband channel model of (4).

#### 4.1. Sources of PLL Output Phase Ambiguity

In order for the proposed carrier synchronization system to be effective, it is important to ensure that there are no potential sources of output phase ambiguity in the PLLs. This section describes three potential sources of phase ambiguity in the proposed two-source carrier synchronization system and suggests practical methods for their mitigation.

##### 4.1.1. Phase Detector Selection

The first potential source of PLL output phase ambiguity is a consequence of the choice of phase detector in each PLL. For example, the common four-quadrant multiplier or XOR phase detectors can lock at a relative phase shift (at the internal frequency of the PLL) of  $\pm\pi/2 + k2\pi$  for  $k \in \mathbb{Z}$ . This phase ambiguity can lead to destructive combining at the destination if one PLL chain were to achieve lock at different phases than the other PLL chain. Fortunately, this sort of phase ambiguity can be eliminated by using a phase-frequency detector [8]. The phase-frequency detector is commonly used in modern PLL circuits and avoids destructive phase ambiguities by locking only at relative phase shifts of  $k2\pi$  at the PLL's internal frequency.

##### 4.1.2. Digital Counter Synchronization

The second potential source of output phase ambiguity is a consequence of the structure of the frequency synthesis PLL. A frequency-synthesis PLL is typically realized by using digital counters to divide the VCO output and input frequencies to a common internal frequency [8]. Output phase ambiguity can result if the counters in PLL chain  $D \rightarrow S_1 \rightarrow S_2$  are not synchronized with those in PLL chain  $D \rightarrow S_2 \rightarrow S_1$  since the output phase of the PLL (with respect to the input phase) directly depends on the state of the digital counters.

One solution to this source of phase ambiguity is to perform integer- $N$  frequency synthesis by avoiding input frequency division, i.e., set  $M = 1$ . In this case, the PLL will generate  $N$  phase-locked output periods for each input period and the potential for phase ambiguity at the output of the PLL is eliminated. In cases where integer- $N$  frequency synthesis is impractical and fractional  $N/M$  synthesis is required, additional synchronization information may need to be occasionally transmitted in the beacon signals in order to establish and maintain counter synchronization.

##### 4.1.3. Oscillator Center Frequency Inaccuracy

A third potential source of phase ambiguity may result from oscillator center frequency inaccuracy in the PLLs. Specifically, if the center frequency  $\omega_q$  of the PLL's VCO is not identical to the desired output frequency  $\omega_{out}$ , the PLL must generate a non-zero mean control voltage at the output of the loop filter in order to drive the VCO to the desired frequency. Given a linear VCO operating characteristic  $\omega = \omega_q + K_0 v_c$ , where  $\omega$  is the actual VCO output frequency and  $v_c$  is the VCO control voltage, we can write the control voltage required to achieve frequency lock as

$$v_c = (\omega_{out} - \omega_q) K_0^{-1}.$$

Assuming that the DC gain of the loop filter is finite<sup>1</sup>, a non-zero mean control voltage implies that the mean phase-detector output voltage must also be non-zero. Given a linear phase-detector characteristic of  $v_p = K_d(\theta_{in} - \theta_{out} - \theta_{lock})$ , where  $v_p$  is the mean phase-detector output voltage and  $\theta_{in}$ ,  $\theta_{out}$ , and  $\theta_{lock}$  are the input phase, output phase, and nominal lock phase, respectively, we can write

$$\theta_{\Delta} := \theta_{in} - \theta_{out} - \theta_{lock} = \frac{\omega_{out} - \omega_q}{K_0 K_d |F(0)|} \quad (5)$$

where  $\theta_{\Delta}$  is the internal phase deviation from the nominal lock phase and  $|F(0)|$  is the DC gain of the loop filter. The resulting carrier phase offset at the destination can be expressed as

$$\phi_{\Delta} = \frac{N_1 N_2}{M_2} (\theta_{\Delta 21} - \theta_{\Delta 11}) + N_2 (\theta_{\Delta 12} - \theta_{\Delta 22}) \quad (6)$$

where  $\theta_{\Delta ij}$  is the internal phase deviation (5) of the  $ij$ th PLL due to oscillator center frequency inaccuracy.

In order to analyze the effect of oscillator inaccuracy on the performance of the two-source carrier synchronization system, we can model the center frequency of each VCO as an independent uniformly distributed random variable centered at the desired output frequency, i.e.,

$$\omega_q \sim \mathcal{U}(\omega_{out}(1 - \rho \cdot 10^{-6}), \omega_{out}(1 + \rho \cdot 10^{-6}))$$

where  $\rho$  represents the parts-per-million (PPM) rating of the oscillator. Under this model, the internal PLL phase deviations are distributed as

$$\theta_{\Delta} \sim \mathcal{U}\left(-\frac{\omega_{out}\rho}{|F(0)|K_0K_d10^6}, \frac{\omega_{out}\rho}{|F(0)|K_0K_d10^6}\right).$$

The exact distribution of  $\phi_{\Delta}$  in (6) is somewhat tedious to compute under this model. We can instead apply a Gaussian approximation for  $\phi_{\Delta}$  by matching the mean and the variance of the Gaussian random variable to that of  $\phi_{\Delta}$ . The mean of  $\phi_{\Delta}$  can be shown to be equal to zero and the variance can be calculated as

$$\sigma^2 := E[\phi_{\Delta}^2] = \frac{N_1^2 N_2^2 \omega_0^2}{3|F(0)|^2 M_1^2 M_2^2 10^{12}} \sum_{ij} \frac{N_j^2 \rho_{ij}^2}{K_{0ij}^2 K_{dij}^2}. \quad (7)$$

<sup>1</sup>We note that, although the loop filter of (1) has infinite gain at DC, practical loop filters will have finite DC gain.

Given  $\phi_{\Delta} \sim \mathcal{N}(0, \sigma^2)$ , the mean carrier power at the destination can be explicitly computed as

$$E \left[ \frac{a_1^2 + 2a_1a_2 \cos(\phi_{\Delta}) + a_2^2}{2} \right] = \frac{a_1^2 + 2a_1a_2 e^{-\frac{\sigma^2}{2}} + a_2^2}{2}.$$

Figure 4 plots theoretically predicted and simulated mean received power as a function of the standard deviation  $\sigma$  of the carrier phase offset  $\phi_{\Delta}$ . We note that the Gaussian approximation tends to be quite accurate for small values of  $\sigma$  and that a 10 degree standard deviation in the carrier phase offset corresponds to approximately a 1% loss in received power with respect to the ideal case.

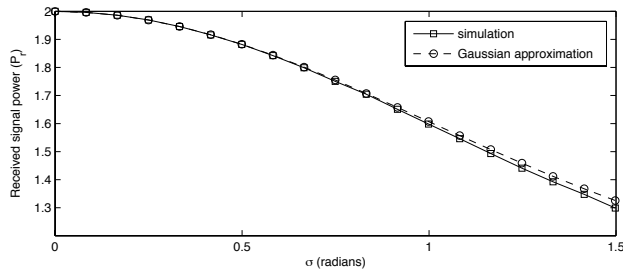


**Fig. 4.** Mean received power of the coherently combined received signal ( $a_1 = a_2 = 1$ ) as a function of the standard deviation of the carrier phase offset.

#### 4.2. Full-Duplex Secondary Beacon Signaling

A potential practical limitation in the proposed system may arise due to the limitations of echo cancelers in wireless transceivers. In the system shown in Figure 1, each source is simultaneously transmitting and receiving a secondary beacon signal at frequency  $\omega_1$ . Imperfect echo cancellation may cause the received secondary beacons to be severely distorted. One possible solution to this limitation is to use different secondary beacon frequencies. It can be shown that, as long as the internal frequencies of each PLL pair PLL11/PLL21 and PLL12/PLL22 are identical, the digital counters used for frequency division are properly synchronized (as discussed in Section 4.1.2), and the channels are single-path, the phase delay through each PLL pair will be identical and carrier signals from each source will coherently combine at the destination. Digital counter synchronization may be somewhat more complicated in this case, however.

Another possible solution to this problem is to time-divide the secondary beacon transmissions (on a single frequency) so that only one source is transmitting at any given time. During intervals when the secondary beacon signal is not present at a source, the secondary PLL at this source will enter a “holdover” mode until the beacon signal is detected again. The duration of the beacon transmissions is a design parameter that is influenced by the time-to-lock of each PLL and the amount of mobility in the system. We also note that time-division of the secondary beacons could potentially be used to maintain synchronization of the PLL digital counters, as discussed in Section 4.1.2.

## 5. CONCLUSIONS

This paper describes an explicit method for synchronizing the carriers of two sources in a cooperative communication system with one destination. Unlike the prior work in this area, the approach described in this paper allows for source and/or destination mobility. The performance of the proposed carrier synchronization system was investigated for three channel models: time-invariant single-path, time-varying single-path, and slowly time-varying Ricean multipath. Our results show that the proposed carrier synchronization system is effective in both time-invariant and time-varying single-path channels. Our results also explicitly show how the performance of the system degrades from the single-path case to the general multipath case where the channel has a large number of reflections. Practical considerations including potential sources of PLL phase ambiguity and methods for avoiding full-duplex secondary beacon signaling were also discussed.

## 6. REFERENCES

- [1] A. Sendonaris, E. Erkip, and B. Aazhang, “Increasing uplink capacity via user cooperation diversity,” in *Proc. 1998 IEEE International Symp. on Information Theory*, Cambridge, MA, August 16-21 1998, p. 156.
- [2] J.N. Laneman and G.W. Wornell, “Energy-efficient antenna sharing and relaying for wireless networks,” in *Proceedings of the IEEE Wireless Communications and Networking Conference*, Chicago, IL, September 2000, pp. 7–12.
- [3] A. Sendonaris, E. Erkip, and B. Aazhang, “User cooperation diversity — part I: System description,” *IEEE Transactions on Communications*, vol. 51, no. 11, pp. 1927–1938, November 2003.
- [4] A. Sendonaris, E. Erkip, and B. Aazhang, “User cooperation diversity — part II: Implementation aspects and performance analysis,” *IEEE Transactions on Communications*, vol. 51, no. 11, pp. 1939–1948, November 2003.
- [5] J.N. Laneman and G.W. Wornell, “Distributed space-time-coded protocols for exploiting cooperative diversity in wireless networks,” *IEEE Transactions on Information Theory*, vol. 49, no. 10, pp. 2415–2425, October 2003.
- [6] G. Barriac, R. Mudumbai, and U. Madhoo, “Distributed beamforming for information transfer in sensor networks,” in *Information Processing in Sensor Networks (IPSN), Third International Workshop*, Berkeley, CA, April 26-27 2004.
- [7] Y.S. Tu and G.J. Pottie, “Coherent cooperative transmission from multiple adjacent antennas to a distant stationary antenna through AWGN channels,” in *Proceedings of the IEEE Vehicular Technology Conference (VTC)*, Spring 2002, vol. 1, pp. 130–134.
- [8] R.E. Best, *Phase-Locked Loops : Design, Simulation, and Applications*, McGraw-Hill, New York, 2003.
- [9] P.Z. Peebles, *Probability, Random Variables, and Random Signal Principles*, McGraw-Hill, New York, 1993.